Electromigration and Thermomigration in Pb-Free Flip-Chip Solder Joints

Chih Chen,[1,*] H.M. Tong,[2] and K.N. Tu[3,*]

[1]Department of Materials Science and Engineering, National Chiao Tung University, Hsin-chu, Taiwan 30010, ROC; email: chih@mail.nctu.edu.tw

[2]Central Labs, Advanced Semiconductor Engineering, Inc., Kaohsiung, Taiwan 811, ROC

[3]Department of Materials Science and Engineering, University of California, Los Angeles, California 90095; email: kntu@ucla.edu

Annu. Rev. Mater. Res. 2010. 40:531–55

First published online as a Review in Advance on April 1, 2010

The *Annual Review of Materials Research* is online at matsci.annualreviews.org

This article's doi: 10.1146/annurev.matsci.38.060407.130253

1531-7331/10/0804-0531$20.00

*Corresponding authors

Key Words

microelectronic packaging, diffusion, reliability, current stressing, Joule heating, thermal gradient, underbump metallization

Abstract

Pb-free solders have replaced Pb-containing SnPb solders in the electronic packaging industry due to environmental concerns. Both electromigration (EM) and thermomigration (TM) have serious reliability issues for fine-pitch Pb-free solder bumps in the flip-chip technology used in consumer electronic products. We review the unique features of EM and TM in flip-chip solder bumps, emphasizing the effects of current crowding and Joule heating. In addition, the challenges to a better understanding of EM and TM in Pb-free solders are discussed. For example, the anisotropic nature of Sn microstructure in Pb-free solders can enhance the dissolution rates of Ni and Cu in solders driven by EM and TM.

1. INTRODUCTION

EM: electromigration
TM: thermomigration
TSV: through-Si-via

Electromigration (EM) has been the most persistent reliability issue in the Al and Cu interconnect technology of microelectronic devices (1). Only recently has EM in flip-chip solder joints in the packaging technology of consumer electronic products been recognized as a reliability issue because such solders fail more easily in comparison to Al and Cu interconnects. Thermomigration (TM) has not been a concern in Al and Cu interconnect technology; however, as with EM, TM is now recognized as a serious reliability problem in flip-chip solder joints. In this review, we explain why EM and TM are critical reliability issues and the unique role of EM and TM in flip-chip solder joints, especially for Pb-free solders.

EM is the mass transportation of a flux of atoms driven by the momentum exchange between a high density of moving charge carriers and diffusing atoms. The drifting electrons collide with the diffusing atoms, causing them to exchange positions with neighboring vacancies in the direction of electron flow. This results in the accumulation of atoms on the anode end and vacancies on the cathode end of the interconnection. Such behavior can lead to hillock and void formation, which can become short and open failures, respectively. Due to the relentless drive to miniaturize microelectronic devices, flip-chip solder joints in the packaging technology used for these devices are increasingly being scaled down. Flip-chip solder bumps with a nominal diameter of 100 μm are being reduced to 25 μm (2). In particular, such tiny solder bumps are required to connect Cu vias in through-Si-via (TSV) technology in stacking chips (3). As a result, the current density in solder joints rises continuously with each generation, making EM a critical reliability issue in electronic packaging technology (4–7). However, in addition to current density, the flip-chip configuration has a built-in effect of current crowding on accelerated EM that is unique and is discussed below.

Due to environmental concerns, the microelectronics industry is moving to Pb-free solders. Most Pb-free solders are Sn-based alloys, and thus EM in Sn-based solders has attracted much attention because of poor field data availability (8). The test standard for EM in solder joints was amended in 2008 (9). This device is called a flip chip because the transistors and the very large scale integration of interconnects are on the bottom side of the chip. Thus, the chip is flipped and connected to the packaging substrate by an array of solder bumps. To see the solder bumps, we can either make a cross section of the sample or take an X-ray tomographic image. **Figure 1*b*** is a synchrotron radiation X-ray tomographic image of a flip-chip sample that shows an array of

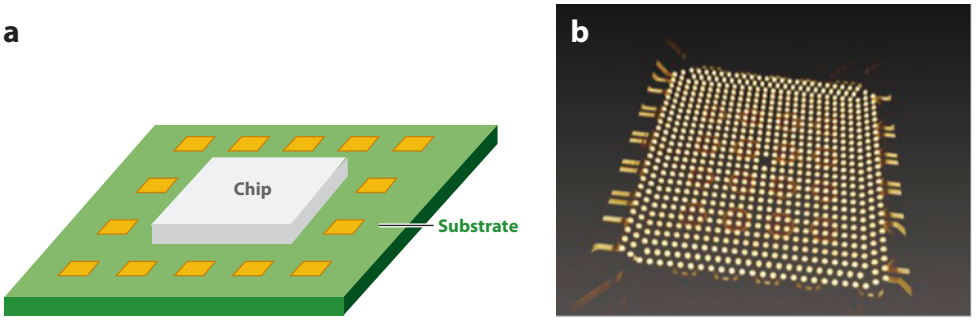

Figure 1

(*a*) The schematic diagram of a flip chip on a substrate. The small squares on the substrate are the electrical contact pads. (*b*) Synchrotron radiation X-ray tomographic image of the sample, showing an array of solder bumps. The synchrotron radiation X-ray tomographic image is courtesy of Ms. Tian Tian at University of California, Los Angeles, and Dr. Alastain Macdowell at Advanced Light Source/Lawrence Berkeley National Laboratory. The flip-chip sample is courtesy of Dr. Yi-Shao Lai at Advanced Semiconductor Engineering, Taiwan, ROC.

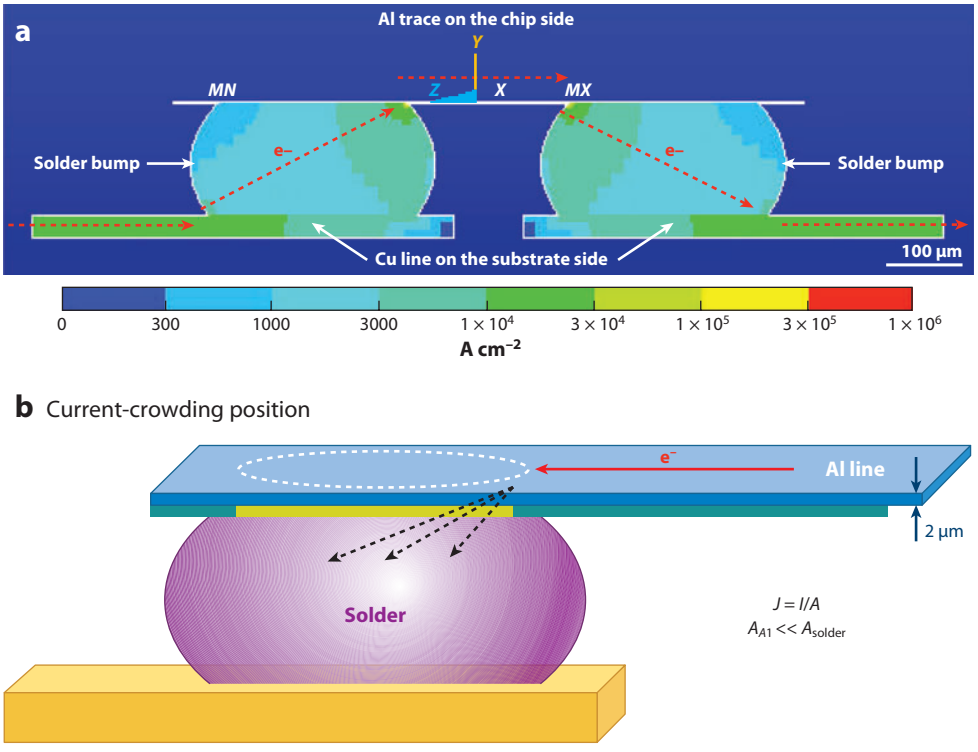

Figure 2

(*a*) Cross-sectional view showing the current-crowding effect in solder bumps during current stressing. Peak current density occurs at the current entrances of the Al trace into the solder bump. (*b*) Three-dimensional schematic diagram depicting the unique line-to-bump configuration of the Al thin film and one of the solder bumps.

solder bumps. Due to differences in the mass absorption of X-rays, we see the solder bumps and part of the Cu lines on the substrate, but not the Si chip or the polymer substrate.

If we consider a pair of solder bumps, we can create, as depicted in **Figure 2*a***, a schematic diagram of their cross section. On the top, or chip side, there is a short Al thin film interconnect connecting the two bumps, whereas on the bottom side, each bump has a thick Cu line connecting it to other bumps or to the outside circuit. **Figure 2*b*** is a three-dimensional schematic diagram depicting the unique line-to-bump configuration of the Al thin film and one of the solder bumps.

The cross section of the Al line on the chip side is at least two orders of magnitude smaller than that of the solder bump. Thus, there is a very large current-density change at the contact between the bump and the line because the same current is passing through them, resulting in current crowding. Current crowding has two significant effects. First, there is an abrupt change in the current density in the Al interconnect where the current turns from the Al line into the solder bump. Second, the current density in the solder bump near the entrance point is approximately one order of magnitude higher than the average current density in the middle of the bump or approximately 10^5 A cm^{-2} near the entrance when the average current density in the middle of the bump is 10^4 A cm^{-2}. This high current density in the current-crowding region causes damage in the solder joints.

2. ELECTROMIGRATION-INDUCED FAILURE IN FLIP-CHIP SOLDER JOINTS

2.1. Current Crowding in Flip-Chip Solder Joints

Figure 3 further illustrates this current-crowding effect. **Figure 3*a*** depicts a three-dimensional simulation of this effect. Panels *b* and *c* of **Figure 3** depict the two-dimensional current distribution in the solder bump from a side view and a top view, respectively. The position of the connecting Al trace is labeled in the figure. Most of the current enters the bump through a small area in the contact opening adjacent to the Al trace. **Figure 3*d*** indicates that the peak current density at the entrance point of the solder bump is 5.1 $\times$ 10^4 A cm^{-2}, whereas the current density is as low as

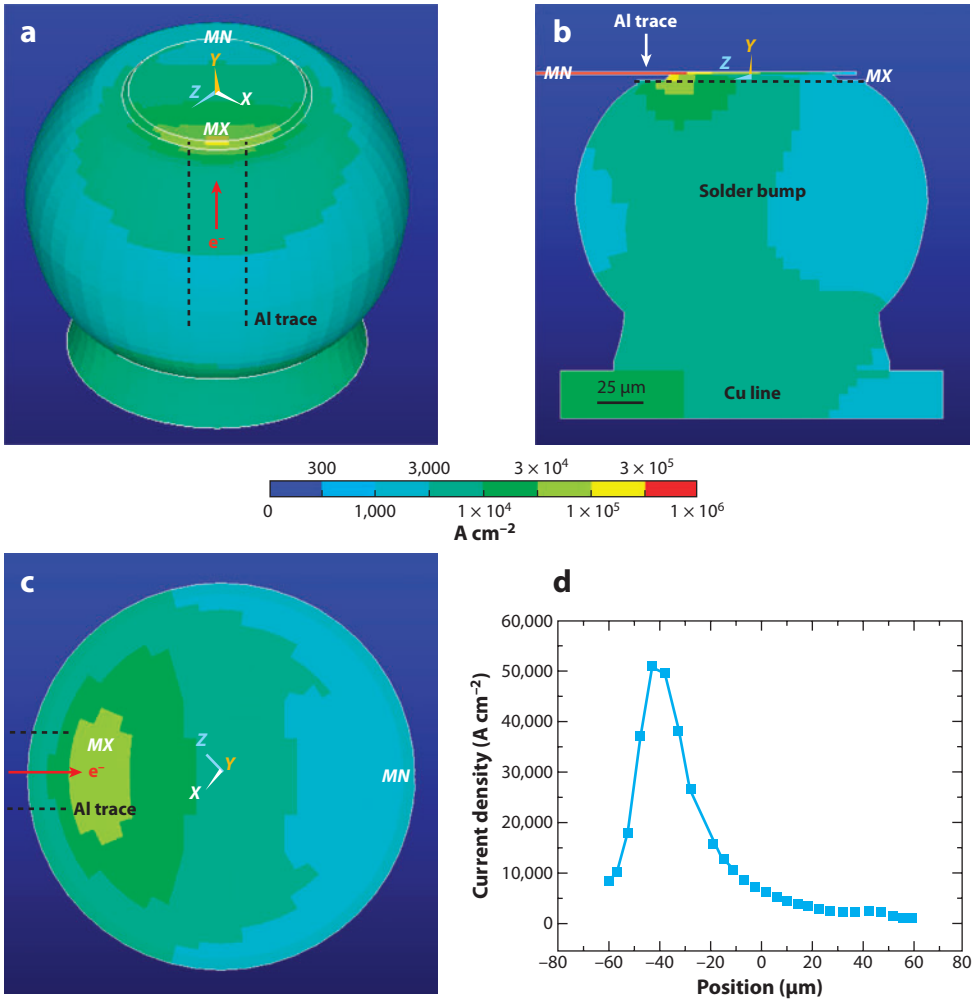

Figure 3

(*a*) Tilt view of the simulated current-density distribution over an entire solder bump when the joint is stressed at 0.6 A at 100°C. The current-density distribution in the solder bump from (*b*) a cross-sectional view and (*c*) a top view. (*d*) The values of current density along the dashed line in panel *b*.

1.1 × 10^3 A cm^{-2} on the other end of the contact opening. Thus, current crowding occurs in flip-chip solder joints.

Consequently, EM damage in a flip-chip solder joint occurs near the cathode contact on the chip side, i.e., the contact between the interconnect and the bump where the electrons flow into the bump (10–21). EM-induced damage begins by void formation near the entrance point of the electric current. The void propagates into the shape of a pancake across the contact. When the void eclipses the entire contact, the flip-chip joint fails.

SEM: scanning electron microscopy

UBM: underbump metallization

2.2 Electromigration-Induced Failure in Flip-Chip Solder Joints

Figure 4*a* depicts a scanning electron microscopy (SEM) image of the cross section of a daisy chain on flip-chip solder joints between a Si chip on the top and a substrate at the bottom. The underbump metallization (UBM) on the Si chip side consisted of Cu/Ni(V)/Al, with 0.8 μm Cu, 0.32 μm Ni(V), and 1 μm Al. The bond pad on the substrate side consisted of Au/Ni(V)/Cu, with 0.08–0.2 μm of Au, 3.8–5 μm of Ni(V), and 38 μm of Cu. The solder bump composition was either eutectic SnPb or 95.5Sn4Ag0.5Cu. The tests were carried out at 50°C with an applied current of 1.7 A for the SnPb solder bumps and 1.8 A for the SnAgCu bumps such that the average current densities in the bump were approximately 3.5 × 10^3 to 3.7 × 10^3 A cm^{-2} (22).

Figure 4*b* depicts an SEM image of three pancake-type contact voids. The failure mode is unique due to the flip-chip configuration: Void formation occurs only at the cathode contact on the Si chip side. Hence, voids or failures occur in only one of a pair of bumps, not in every bump. Kinetic analysis on a two-dimensional model of pancake-type void growth has been published (22). No model of three-dimensional growth has been reported, and such a model may emerge only after in-situ X-ray tomographic observation of three-dimensional growth.

In **Figure 5**, a schematic diagram depicts the cross section of a solder joint with a pancake-type void formation at the upper interface. The formation and propagation of the void displaced the entrance of the electron current to the front of the void. Therefore, void formation has little effect

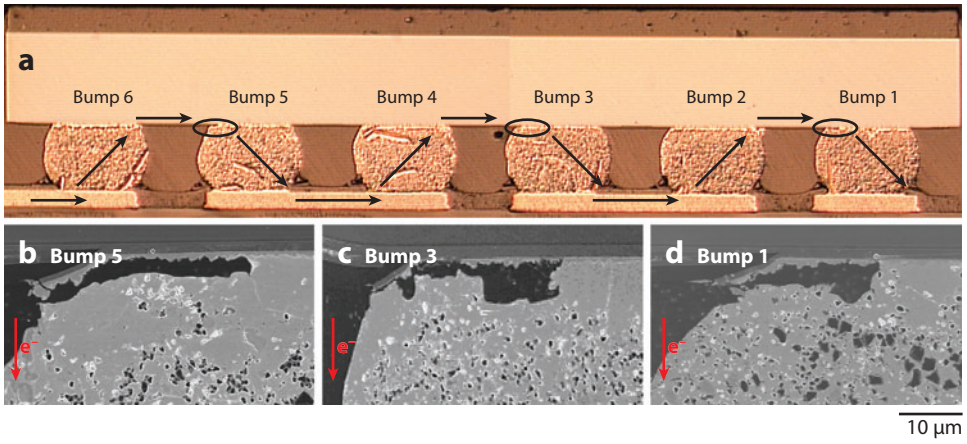

Figure 4

(*a*) Scanning electron microscopy (SEM) cross sections showing the location of void formation (*odd-numbered bumps*, *upper left corner*). The electron flow is indicated by the arrows. The cathode contacts on the Si where the electron current enters the solder bump are indicated by small circles. (*b*) Enlarged SEM image of the voids in bump 5. (*c*) Enlarged SEM image of the voids in bump 3. (*d*) Enlarged SEM image of the voids in bump 1.

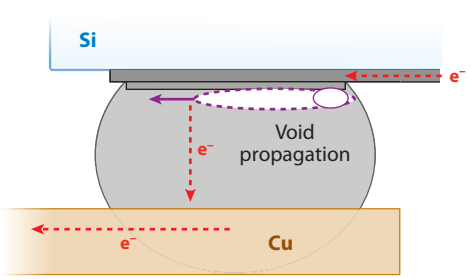

Figure 5

A schematic diagram of a cross section of a solder joint with pancake-type void formation at the upper interface.

on the resistance of the solder bump as long as the current can enter into the solder bump (23, 24). Finally, an abrupt change in resistance occurs when the void has extended across the entire joint or when the contact becomes open (25–52). **Table 1** compares the electrical behavior between Al (or Cu) interconnects and solder joints. The resistance of a cubic piece of solder 100 μm × 100 μm × 100 μm in size (the size of a solder joint) is approximately 1 mΩ. The resistivities of Sn and Pb are 11 μΩ-cm and 22 μΩ-cm, respectively. The resistance of an Al or Cu line of length 100 μm with a cross section of 1 μm × 0.2 μm is approximately 10 Ω. The solder joint is a low-resistance conductor, but the interconnect is a high-resistance conductor that becomes the source of Joule heating. Because the conducting path in Al extends due to growth of the pancake void, Joule heating increases with such growth (23). Joule heating can lead to TM in flip-chip solder joints, which is discussed below. Sometimes Joule heating can be large enough to melt the solder bump (48, 50) in a time-dependent manner (45).

3. THERMOMIGRATION IN FLIP-CHIP SOLDER JOINTS

3.1. Joule Heating and Temperature Distribution in Flip-Chip Solder Joints

Joule heating is waste heat generated by entropy production, which is given as (52)

$$\frac{T\,dS}{V\,dt} = j^2\rho, \qquad 1.$$

where T, S, V, and t are temperature, entropy, volume, and time, respectively. ds/dt is the rate of entropy production, and j and ρ are current density (A cm^{-2}) and resistivity (μΩ-cm), respectively.

Table 1 Comparison of the electrical behavior between Al (or Cu) interconnects and solder joints

	Al or Cu interconnects	Solder bumps
Cross section	0.5 × 0.2 μm^2	100 × 100 μm^2
Resistivity	1.7–2.6 μm·cm	11.5–22 μm·cm
Resistance	1–10 Ω	10^{-3} Ω
Current	10^{-3} A	1 A
Current density	10^6 A cm^{-2}	10^3–10^4 A cm^{-2}

Usually, the heating power, P, is described by the Joule heating relationship as

$$P = I^2 R = j^2 \rho V . \quad 2.$$

I is the applied current, and $I/A = j$, where A is the cross-sectional area of the conductor, R is the resistance of the entire conductor and $R = \rho l/A$, l is the length of the conductor, and $V = Al$. Thus, $P = I^2R$ is the Joule heating per unit time of the entire conductor, and $j^2\rho$ is the Joule heating per unit volume per unit time of the conductor.

As a point of reference to better understand Joule heating in an Al interconnect and a solder bump in a flip-chip device, the resistance of an Al trace is typically hundreds of milliohms (14), whereas it is approximately 7 mΩ for a solder bump (53) and tens of milliohms for the Cu lines on the substrate side. Considering Joule heating per unit volume for Al, if we take $j = 10^6$ A cm^{-2} and $\rho = 10^{-6}$ Ω-cm, then Joule heating is $\rho j^2 = 10^6$ J cm^{-3} s^{-1}. For the solder, if we take $j = 10^4$ A cm^{-2} and $\rho = 10^{-5}$ Ω-cm, then Joule heating is $\rho j^2 = 10^3$ J cm^{-3} s^{-1}. Therefore, the Al trace on the chip side serves as the major contributor to Joule heating, causing the side of the solder bump at the chip side to be hotter than that on the substrate side.

Nonsymmetrical Joule heating takes place during EM tests due to current crowding (54–58). As shown in **Figure 6**, the temperature distribution in the solder joints was obtained using thermoelectrical finite element simulation (23, 59). The figure shows the Al trace, solder bumps,

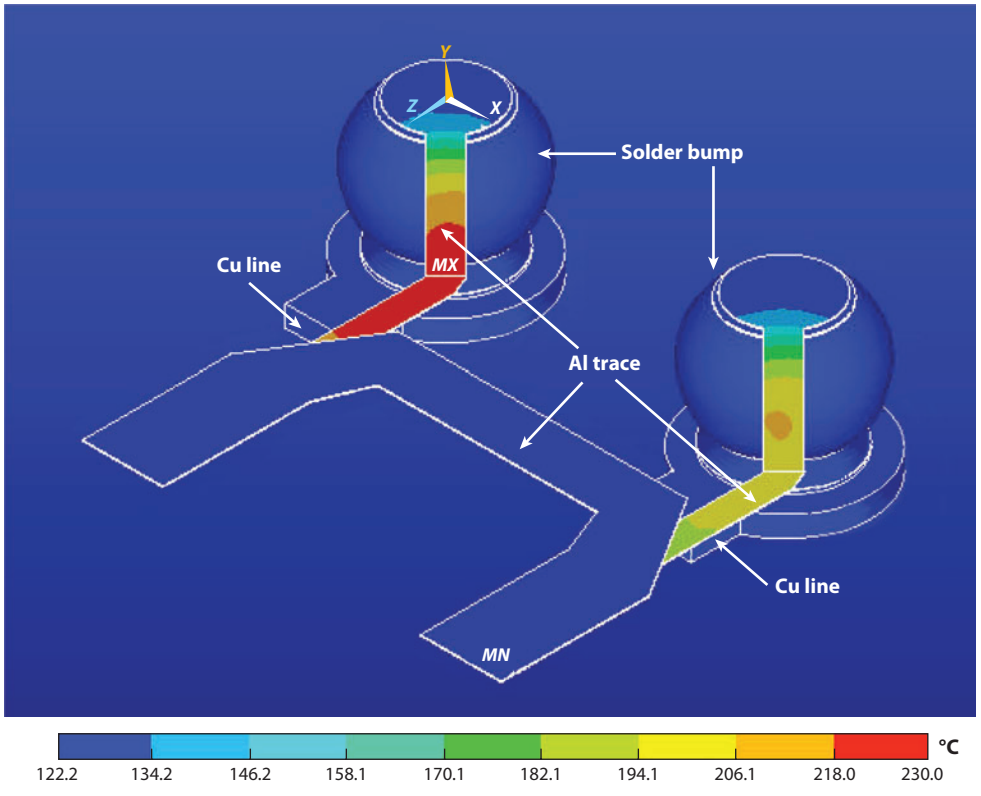

Figure 6

Three-dimensional simulation of the temperature distribution for two solder joints subjected to 0.6-A current stressing with the substrate maintained at 100°C. The peak temperature occurs at the Al trace because it has a higher resistance than the solder bumps and the Cu line and has local Joule heating.

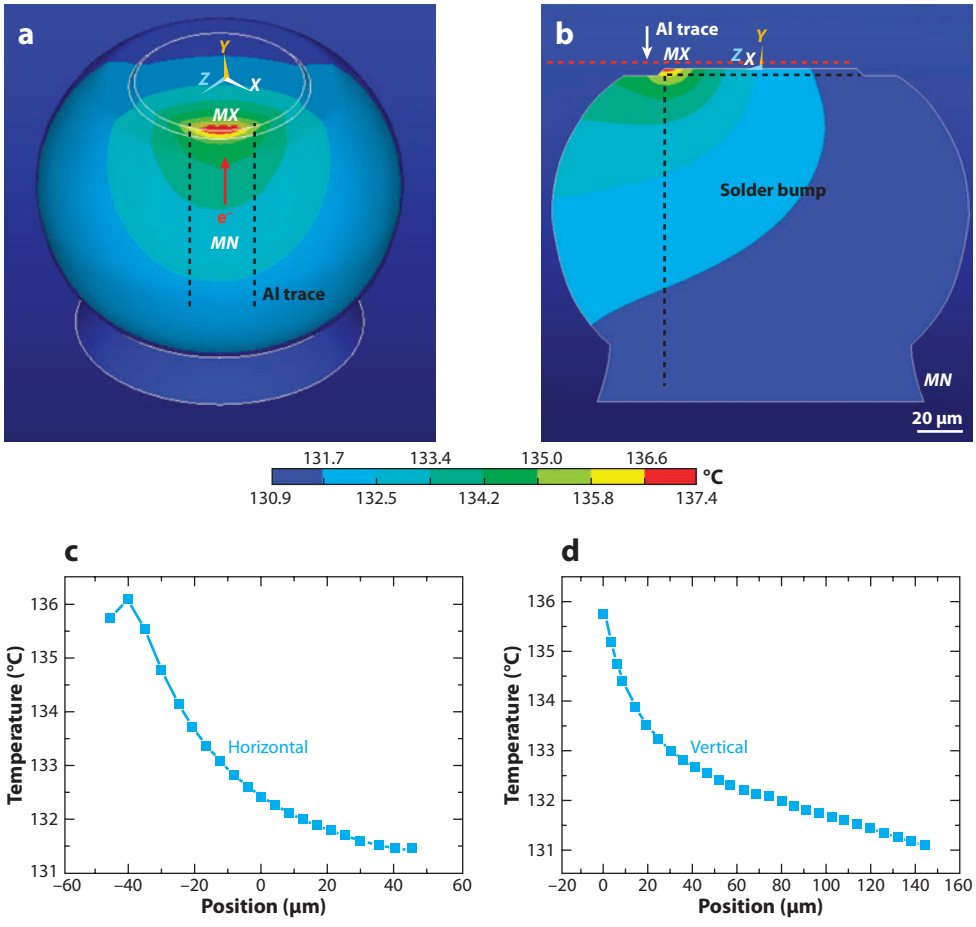

Figure 7

(*a*) Tilt view of the simulated temperature distribution over an entire solder bump when the joint is stressed at 0.6 A at 100°C. (*b*) Cross-sectional view showing the temperature distribution. A hot spot is observed at the current entrance from the Al trace. (*c*,*d*) The temperature profiles along (*c*) the black horizontal dashed line and (*d*) the black vertical dashed line in panel *b*. The red horizontal dashed line denotes the position of the Al trace in panel *b*.

and the Cu line. Two solder bumps were powered by 0.6 A through the circuit shown in the figure. The Al trace is the hottest component in the joint because its local current density is approximately two orders of magnitude larger than that in the solder and in the Cu line in the substrate. The maximum temperature (~230°C) occurs at the Al trace. Because the local current density in the solder is much lower and the solder has a larger volume to dissipate heat, the temperature in the solder bump decreases to approximately 137°C. **Figure 7*a*** shows the simulated temperature distribution in the solder bump only. A hot spot exists at the entrance point of the current from the Al trace. **Figure 7*b*** illustrates a cross-sectional view of the temperature distribution inside the solder, showing the existence of the hot spot in the solder adjacent to the entrance point where the current from the Al trace enters the solder at the contact opening. The hot-spot location almost overlaps with the location of the current-crowding region, as shown before.

The temperature at the spot is 137.4°C, which is 5.6°C higher than the average value in the solder. A hot spot is evident. The temperature on the chip side is higher than that on the substrate side. **Figure 7*c*** illustrates the temperature profile along the horizontal dashed line in **Figure 7*b***, and **Figure 7*d*** illustrates the temperature profile along the vertical dashed line in **Figure 7*b***. The thermal gradient here is denoted as the subtraction of the temperature in the hot spot by the temperature at the opposite end of the solder, which is then divided by the distance between the two locations. Under this stressing condition, the vertical thermal gradient is calculated to be 323°C cm^{-1}, whereas the horizontal thermal gradient is calculated to be 510°C cm^{-1}. The current density in the Al trace is 1.2×10^6 A cm^{-2}. The average current density in the solder joint is 5.3×10^3 A cm^{-2} on the basis of the contact opening. In the hot spot, the maximum current density is 1.1×10^5 A cm^{-2}, whereas the average current density involved in a volume of 5 μm × 5 μm × 5 μm is estimated to be 9×10^4 A cm^{-2}. In this simulation model, the total resistance of the Al trace is approximately 1331 mΩ, and the resistance of the solder bump is approximately 10 mΩ. Therefore, the Al trace generates most of the heat.

Infrared microscopy has recently been used to verify the simulation results of the hot spot (58). The temperature distribution can be examined in a cross-sectioned bump during current stressing. **Figure 8*a*** shows the measured temperature map in a 150-μm-diameter SnAg solder bump when the stressing current is 0.6 A. A hot spot is clearly observed at the upper-right corner, where the current crowds into the solder bump. The temperature differences are 5.5°C and 16.7°C along the horizontal line and the vertical line in **Figure 8*a***, respectively. The temperature profiles along the two lines are depicted in **Figure 8*b*,*c***. A huge thermal gradient of 2392°C cm^{-1} develops across the solder bump. The Joule heating effect also establishes a horizontal thermal gradient of 786°C cm^{-1}.

Figure 9*a* depicts a plot of the average and hot-spot temperatures as a function of applied current densities or applied current for a SnAg solder bump with a 5-μm Cu/3-μm Ni UBM. The applied current ranged from 0.1 A to 0.6 A as the flip-chip package was placed on a hot stage maintained at 100°C. With higher currents that exceeded 0.6 A, the solder bump tended to melt. As observed in **Figure 9*a***, the average temperature in the solder bump increased from 100°C to 152°C when the bump was subjected to 0.6-A current stressing. Therefore, the Joule heating effect is very significant at higher stressing currents. **Figure 9*b*** shows the built-in thermal gradient as a function of applied current. A thermal gradient of more than 2000°C cm^{-1} can be established if the applied current density is large enough.

3.2. Thermomigration in Unpowered Flip-Chip Composite Solder Joints of SnPb

We discuss above that the applied current in a flip-chip device causes not only EM but also Joule heating. The latter induces a temperature gradient across the solder joint, wherein a sufficiently large temperature gradient (~1000°C cm^{-1}, discussed below) can cause TM. Thus, EM in flip-chip solder joints is accompanied by TM (50, 54, 60–73). To study TM alone, we must decouple the two, as shown below.

Figure 10 shows a depiction of a cross section and an SEM image of a composite 97Pb3Sn and 37Pb63Sn flip-chip solder joint. Composite solder joints have been used to study TM in particular because the large image contrast between Sn and Pb enables us to easily observe the effect of TM on phase change in SnPb solders (60, 74).

As a control experiment, the composite flip-chip samples were heated in an oven at a constant temperature of 150°C and a constant atmospheric pressure for one, two, and four weeks. The microstructures of the sample cross sections were examined with optical microscopy (OM) and

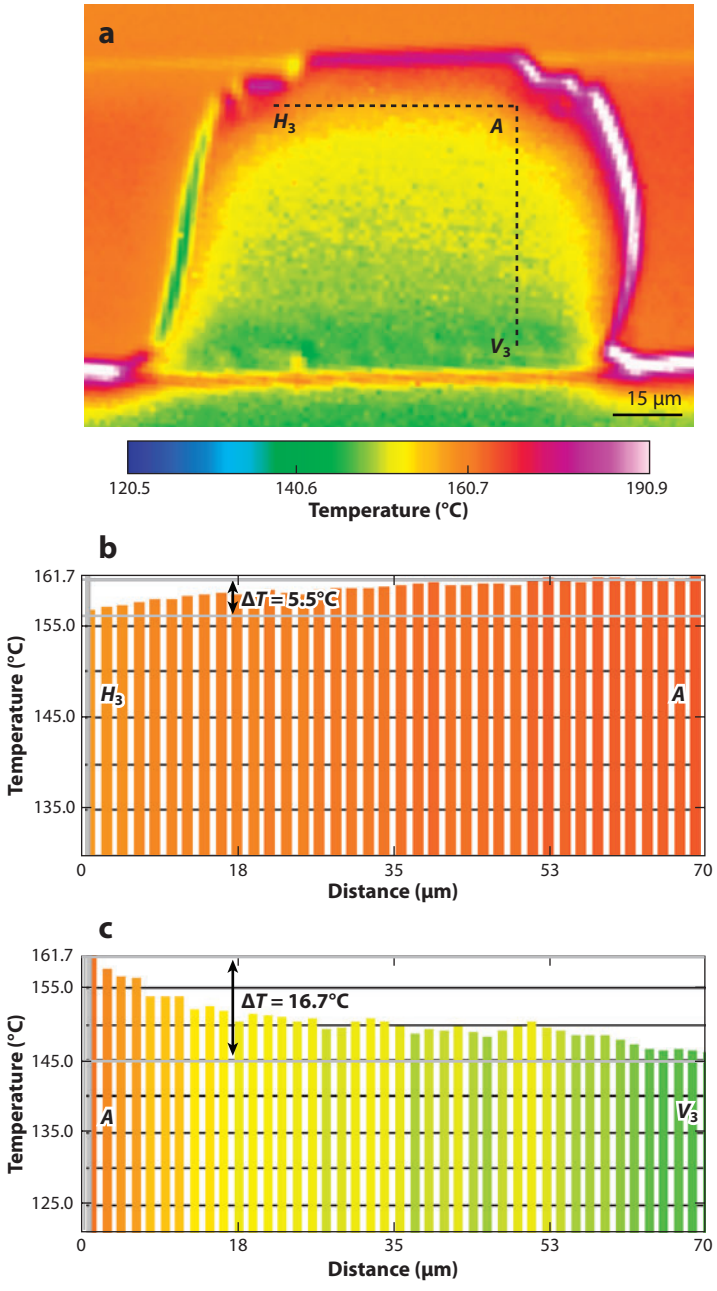

Figure 8

(*a*) The temperature map measured by an infrared microscope when the joint was stressed by 0.6 A. A hot spot is observed on the upper right of the bump, where the current crowds into the solder bump from the Al trace. The temperature differences are 5.5°C and 16.7°C along the horizontal line and vertical line, respectively. (*b*,*c*) The temperature profile along (*b*) the horizontal line and (*c*) the vertical line in panel *a*. The origin of panel *b* was set at point H_3, whereas the origin of panel *c* was set at point *A*. A huge thermal gradient of 2392°C cm^{-1} develops across the solder bump (between points *A* and V_3). The Joule heating effect also establishes a horizontal thermal gradient of 786°C cm^{-1}.

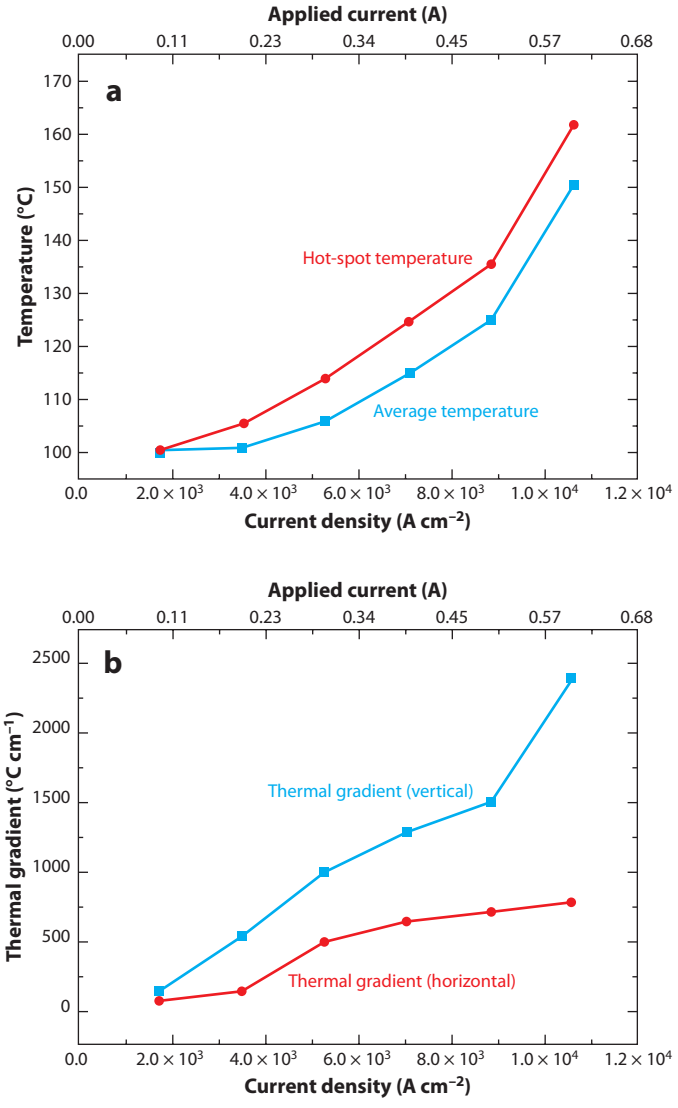

Figure 9

(*a*) Plot of average and hot-spot temperatures as a function of applied current densities or applied current with a 5-μm Cu/3-μm Ni underbump metallization (UBM). The curve shows a parabolic behavior that follows the Joule heating relationship, as described in Equation 2. The average temperature is obtained by averaging the temperature over a 70 μm × 70 μm area in the center of the solder bump. (*b*) The resultant thermal gradient as a function of applied current. The thermal gradient may be more than 2000°C cm^{-1} when the applied current density is larger than 1×10^4 A cm^{-2}.

SEM. No mixing between the high Pb and the eutectic SnPb was observed, and the image was essentially unchanged, just as in **Figure 10*b***. No observed phase mixing can be explained by the negligible chemical potential difference between high Pb and eutectic SnPb at a constant temperature of 150°C. In other words, there is neither a chemical potential gradient nor a driving force to move the phases.

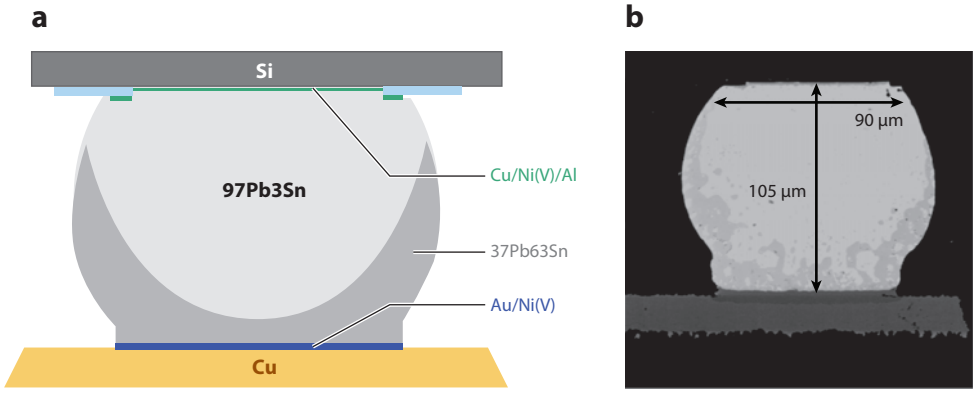

Figure 10

(*a*) A cross section of a composite 97Pb3Sn and 37Pb63Sn flip-chip solder joint. (*b*) Scanning electron microscopy (SEM) image of the cross section. The darker region at the bottom is the eutectic SnPb. The brighter region is the 97Pb3Sn phase.

To induce TM in the composite solder joints, we used the temperature gradient induced by Joule heating in EM. A set of flip-chip samples is depicted in **Figure 11*a***, wherein there are 24 bumps on the periphery of a Si chip, and all the bumps had their original microstructure, as shown in **Figure 10*b***, before EM stressing. After EM was conducted through only four pairs of bumps—pairs 6/7, 10/11, 14/15, and 18/19 in **Figure 11*a***—TM affected all the unpowered solder joints, as shown in **Figure 11*b***. All the Sn migrated to the hot Si side, whereas the Pb migrated to

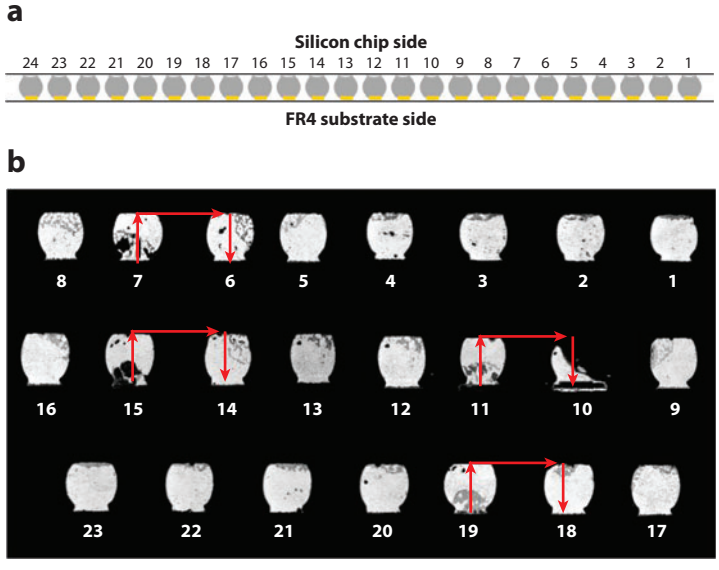

Figure 11

(*a*) Schematic diagram depicting 24 bumps on the periphery of a Si chip. Each bump has its original microstructure, as shown in **Figure 10*b***, before electromigration (EM) stressing. EM was conducted at 1.6×10^4 A cm^{-2} at 150°C through only four pairs of bumps on the chip's periphery: pairs 6/7, 10/11, 14/15, and 18/19. (*b*) Thermomigration (TM) affected all the unpowered solder joints: The darker eutectic phase moved to the hot Si side.

the cold substrate side. The redistribution of Sn and Pb was caused by the temperature gradient across the solder joints because no current was applied to them.

3.3. In Situ Observation of Thermomigration in Flip-Chip Composite Solder Joints of SnPb

In situ observation of TM was conducted with flip-chip samples (**Figure 12*a***). The chip was cut, and only a thin strip of Si was retained. The strip had one row of solder bumps connecting it to the substrate. The bumps were cut and polished to the middle so that the cross section of each bump was exposed for in situ observation during TM. **Figure 12*a*** is a schematic diagram of the Si strip and a row of four cross-sectioned bumps. Due to the excellent thermal conduction of Si and the small strip used, whenever one pair of the bumps is powered by dc or ac current, the other pair of unpowered solder joints experiences almost the same thermal gradient as the powered pair. This set of samples was used to directly observe changes in the cross-sectioned bump surfaces during EM and TM.

The pair of joints depicted on the left side of **Figure 12*a*** was powered at 2×10^4 A cm^{-2} for 20 h at 150°C. The pair of joints on the right had no electric current. Interestingly, both pairs of joints exhibited composition redistribution and damage. The pair on the right (unpowered) showed a uniform void formation at the interface on the top side, i.e., the Si side, which is also the hot side. **Figure 12*b*** shows an SEM image of one of these joints.

In the bulk of the joint, some phase redistribution can be recognized. The redistribution of Sn and Pb can be measured by an electron microprobe from the cross sections of the unpowered pair depicted on the right side of **Figure 12*a***, where Sn has migrated to the hot side and Pb has moved to the cold side. The void formation indicates that TM can cause failure in flip-chip solder joints.

If we assume that there is no temperature gradient in the pair of bumps depicted on the right side of **Figure 12*a***, that is, the bumps have uniform temperature, then the pair's thermal history is similar to that of isothermal annealing. In this way, no phase redistribution or void formation should exist because isothermal annealing has no effect on phase mixing or unmixing in composite solder joints. However, could other driving forces lead to the observed phase change? A good choice aside from electrical and thermal forces is mechanical force, yet mechanical force may also exist in isothermal annealing. Annealing causes interfacial chemical reactions between the solder

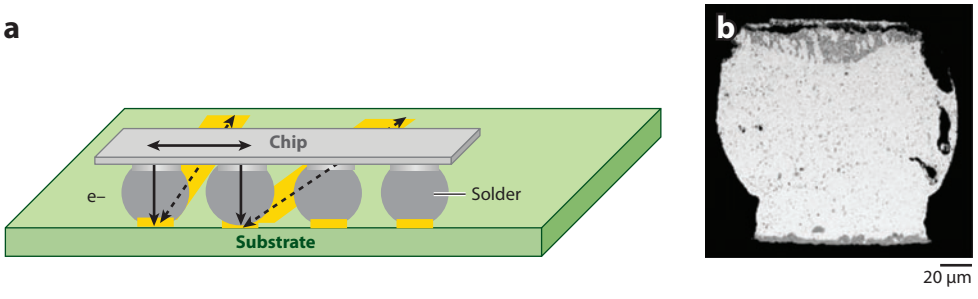

Figure 12

(*a*) A schematic diagram of the Si stripe and a row of four of the cross-sectioned bumps. The chip was cut, and only a thin stripe of Si was retained. The stripe has one row of solder bumps connecting it to the substrate. The bumps were cut in the middle so that the cross section of the bump was exposed for in situ observation during electromigration (EM). The pair of joints on the left was powered at 2×10^4 A cm^{-2} for 20 h at 150°C. The pair of joints on the right had no electric current. All joints showed composition redistribution and damage. (*b*) An SEM image of one of these joints.

and UBM on the chip side, as well as between the solder and bond-pad metal on the substrate side. The growth of intermetallic compounds may generate stress due to molar volume change. Under these assumptions, this effect should have been observed in the sample isothermally annealed at 150°C for four weeks, but no noticeable changes were observed. Furthermore, solders have a very high homologous temperature at 150°C, so it is highly likely for any stress therein to have relaxed over four weeks.

For Pb-free flip-chip solder joints, contrast due to phase change is not as clear as that observed in SnPb solders. We need the marker motion of indented markers on the polished surface of a solder joint to measure the flux of mass motion, making in situ measurements important for Pb-free solders (62, 64, 75).

4. COMPARISON OF ELECTROMIGRATION AND THERMOMIGRATION DRIVING FORCES

For the EM and TM driving forces, we recall that the atomic fluxes driven by them can be given respectively as (72)

$$J_{EM} = C\frac{D}{kT}Z^*eE = C\frac{D}{kT}Z^*e\rho j, \quad 3.$$

$$J_{TM} = C\frac{D}{kT}\frac{Q^*}{T}\left(-\frac{\partial T}{\partial x}\right), \quad 4.$$

where C is concentration, D is atomic diffusivity, kT is thermal energy, Z^* is the effective charge number of EM, e is electron charge, E is the electric field, ρ is the electric resistivity, j is the current density, and Q^* is the transport heat in TM. Q^* has the same dimensions as the chemical potential, μ, so its unit is heat energy per atom. Q^* is the difference between the heat carried by the moving atom and the heat of the atom in the initial state (the hot end or the cold end). On the basis of Equation 4, for the element that moves from the hot end to the cold end, Q^* is positive. For an element moving from cold to hot, Q^* is negative.

The EM and TM driving forces can be given respectively as

$$F_{EM} = Z^*e\rho j, \quad 5.$$

$$F_{TM} = -\frac{Q^*}{T}\left(\frac{\Delta T}{\Delta x}\right). \quad 6.$$

The TM driving force can be estimated by using Equation 6, wherein we take $\Delta T/\Delta x = 1000°\text{C cm}^{-1}$, consider the temperature difference across an atomic jump, and take the jump distance to be $a = 3 \times 10^{-8}$ cm. We have a temperature change of 3×10^{-5} K across an atomic spacing. Thus, the thermal energy change is

$$3k\Delta T = 3 \times 1.38 \times 10^{-23}\,(\text{J/K}) \times 3 \times 10^{-5}\,\text{K} \approx 1.3 \times 10^{-27}\,\text{J}.$$

As a comparison, we consider the driving force, F_{EM}, of EM in Equation 5 at current densities of $1 \times 10^4\,\text{A cm}^{-2}$ and $1 \times 10^8\,\text{A m}^{-2}$, which has induced EM in solder alloys. We take $\rho = 10 \times 10^{-8}$ Ω-m, a Z^* on the order of 10, and $e = 1.602 \times 10^{-19}$ C, resulting in $F = 10 \times 1.6 \times 10^{-19}\,(\text{C}) \times 10 \times 10^{-8}\,(\Omega\text{-m}) \times 10^8\,\text{A m}^{-2} = 1.6 \times 10^{-17}\,\text{C-V m}^{-1} = 1.6 \times 10^{-17}$ N.

The work done by the force at the distance of an atomic jump of 3×10^{-10} m is $\Delta w = 4.8 \times 10^{-27}$ N-m $= 4.8 \times 10^{-27}$ J. This value is close to the thermal energy change we calculated above for TM. Thus, if a current density of $10^4\,\text{A cm}^{-2}$ can induce EM in a solder joint, a temperature gradient of $1000°\text{C cm}^{-1}$ induces TM in a solder joint.

In EM in Al and Cu interconnects, a current density greater than 10^5 to 10^6 A cm^{-2} is typically required. This means that we need a temperature gradient larger than 10,000°C cm^{-1} to provide the same driving force, which is too high. This is why TM has not been a reliability concern in Al and Cu interconnect technology.

IMC: intermetallic compound

With transport heat, Q^* can be positive or negative. In the Fe-C system, C interstitially moves to the hot end with a negative heat of transport (76). In alloys of SnPb, when TM drives Pb to move from the hot end to the cold end, Pb moves down the temperature gradient; however, TM drives Sn to move in the opposite direction, against the temperature gradient. On the basis of Equation 4, the Q^* for Pb is positive, but for Sn the Q^* is negative because Sn moves to the hot end. This may be the result of one temperature gradient in TM for both species. Unlike interdiffusion in a diffusion couple, in which the concentration gradients of the two interdiffusing species are in the opposite direction, the chemical potential change in interdiffusion can be positive for both species.

To measure Q^*, if we know the atomic flux, we can use the flux equation, i.e., Equation 4, when the diffusivity, average temperature, and temperature gradient are known. The molar heat of Pb transport, Q^*_{Pb}, is estimated to be +79 kJ mol^{-1} (60). When Pb is the dominant diffusing species and moves from the hot end to the cold end of the solder bump, Sn will be pushed back in the opposite direction if a constant volume process is assumed. The effect of reverse flux for Sn on the calculation of transport heat in a two-phase microstructure needs to be studied. Marker motion has indicated that, in Pb-free flip-chip solder joints, Sn moves from the cold side to the hot side in TM (64). Why Sn moves against the temperature gradient is unclear, and more systematic studies are needed to clarify this phenomenon.

Although we use unpowered solder bumps next to dc-powered bumps to study TM, we can study dc-powered bumps to ascertain the combined effects of EM and TM. Furthermore, we can use ac-powered bumps to study TM without the interference of EM (62, 64).

5. EFFECT OF Cu UNDERBUMP-METALLIZATION THICKNESS ON CURRENT CROWDING IN FLIP-CHIP SOLDER JOINTS

Due to the unique line-to-bump configuration of flip-chip solder joints, current crowding is the major cause of EM failure. To reduce the effect of current crowding, we can increase the thickness of Cu UBM so that current crowding occurs in the Cu rather than in the solder (77–83). A systematic study was performed to increase the Cu UBM thickness from 0.4 μm to 5 μm, 10 μm, and 50 μm (84). The 50-μm Cu UBM thickness is often referred to as Cu column bumps. Thick Cu enables a redistribution of the current over the entire Cu UBM. Hence, the current density in the solder bump is much closer to the average value, i.e., almost no current crowding occurs in the solder near the Cu/solder interface. Three-dimensional simulations can clarify the effect of current redistribution in the thick Cu and the solder.

In the case of thin Cu, for example, the Cu in the thin-film UBM of Al/Ni(V)/Cu is approximately 0.4 μm, and current crowding occurs in the solder and impacts the EM of the solder. In the thin UBM, all the 0.4-μm Cu is consumed to form intermetallic compounds (IMCs). Typically, EM induces void formation in the solder, and propagation of the pancake-type void occurs at the solder/IMC interface along the contact.

In the case of 5- to 10-μm-thick Cu UBM, most current crowding occurs within the Cu (85). Although part of the current crowding is extended into the solder, the degree of crowding in the solder is small, so the current density in most of the solder joint is quite uniform and close to the calculated average value of current density in the bulk of the solder. The void formation in this case, as shown in **Figure 13**, is located at the entrance of the current to the bump, and the void

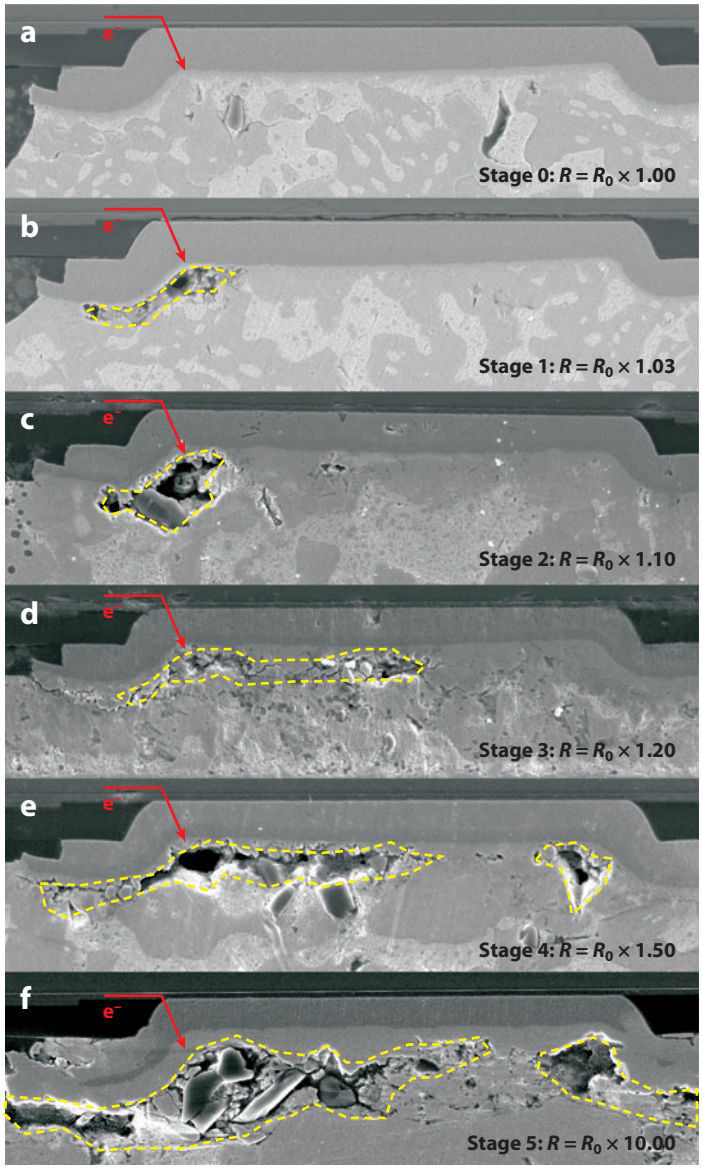

Figure 13

Void formation at different stages of electromigration (EM) when the joints were stressed by 0.8 A at 150°C. (*a*) At 0 h. (*b–f*) Bump resistance increased by a factor of (*b*) 1.03, (*c*) 1.10, (*d*) 1.20, (*e*) 1.50, and (*f*) 10.00.

grows larger with time. EM dissolves the Cu into the solder and reduces the Cu thickness. When the Cu thickness is reduced to 5 μm or below, the failure mode repeats, as discussed above. With time, the interaction between EM and chemical reaction converts Cu into Cu_3Sn and Cu_6Sn_5, and the resistance of the contact subsequently increases quickly and leads to failure.

In the case of a Cu column bump of 50 μm or more in height and in diameter, the bulk part of the solder bump is replaced by the Cu bump, so the remaining solder is approximately 20 μm thick. There is no current crowding in the solder part of the joint. However, a large number of

voids appear in the Cu_3Sn layer; most of them are closer to the Cu_3Sn/Cu interface (82). The thickness of Cu_3Sn and the number of voids increase significantly with increasing current density.

In a solder joint consisting of a limited amount of Sn combined with an infinite amount of Cu, Cu_3Sn grows thicker at the expense of Cu_6Sn_5 and is accompanied by an extensive formation of Kirkendall voids. When one molecule of Cu_6Sn_5 is converted into two Cu_3Sn, it releases three Sn atoms, which attracts nine Cu atoms to form Cu_3Sn. The vacancies that are needed for the Cu diffusion may condense to form voids. Therefore, for a combination of a very thick Cu column bump and a relatively thin solder bump, the Cu_6Sn_5 transforms to Cu_3Sn, and the latter can grow very thick, so the vacancy flux that opposes the Cu flux forms Kirkendall voids. These voids cause the joint to fail mechanically. The effect of these Kirkendall voids on the electrical and thermal conductivity of Cu_3Sn and, in turn, the effect of the void formation on Joule heating and heat dissipation in the solder joint are of great concern and may also affect the temperature gradient in the solder joint. Thus, both EM accompanied by TM and the formation of Kirkendall voids may replace current crowding as a serious reliability issue when Cu column bumps are used.

6. CHALLENGES FOR FUTURE STUDY OF ELECTROMIGRATION AND THERMOMIGRATION IN Pb-FREE FLIP-CHIP SOLDER JOINTS

6.1. Fast Dissolution of Cu and Ni Under Electromigration

Extensive IMC formation may occur during EM and TM in Pb-free solders with Cu UBM (86–96). In particular, for solder joints with Cu columns or with TSV technology, the height of the solder bump may be as low as 20 μm (6). As a result, the entire solder bump may transform completely into Cu-Sn IMCs during current stressing, which may induce brittle fracture (97). The EM behavior of the IMCs may become important due to this brittle fracture. Recently, several studies addressed this issue (97–101). In addition, because many Cu or Ni atoms are dissolved into the solder bumps to form IMCs, the impact of these atoms on the mechanical properties of the joint is of interest. The mechanism by which IMC formation blocks Sn diffusion is unclear, especially where IMCs form near the anode.

A solder joint 20 μm high requires a temperature difference of 2°C across the joint to yield a temperature gradient of 1000°C cm^{-1}. It is not easy to control a temperature difference across a solder joint below 2°C, and hence TM may become a serious reliability issue in small flip-chip solder joints.

6.2. Effect of Sn Grain Orientation on Electromigration and Transmigration

Extrafast Cu and Ni dissolution may take place along specific Sn grain orientations (102). Lu et al. (102) found that rapid depletion of IMCs and Cu UBM occurs along the *c* axis of Sn crystals, resulting in significant damage to the joints. The fast dissolution of Cu and Ni is due to the fact that Cu interstitial diffusivity along the *c* axis is 500 times faster than along the *a* or *b* axis of Sn crystals at 25°C (103), and the diffusivity of Ni along the *c* axis is $\sim 7 \times 10^4$ times that at right angles (*a* or *b* axis) at 120°C (104). Therefore, Sn grain orientation plays an important role in the EM and TM of Sn-based Pb-free solders. More effort is needed to provide a better understanding of this interesting phenomenon of anisotropic diffusion.

6.3. Stress Migration in Solder Bumps

Several researchers have proposed that stress in solder exists during current stressing (105–110). Built-in stress may relate to the current-crowding effect. Panels *a–e* of **Figure 14** show the

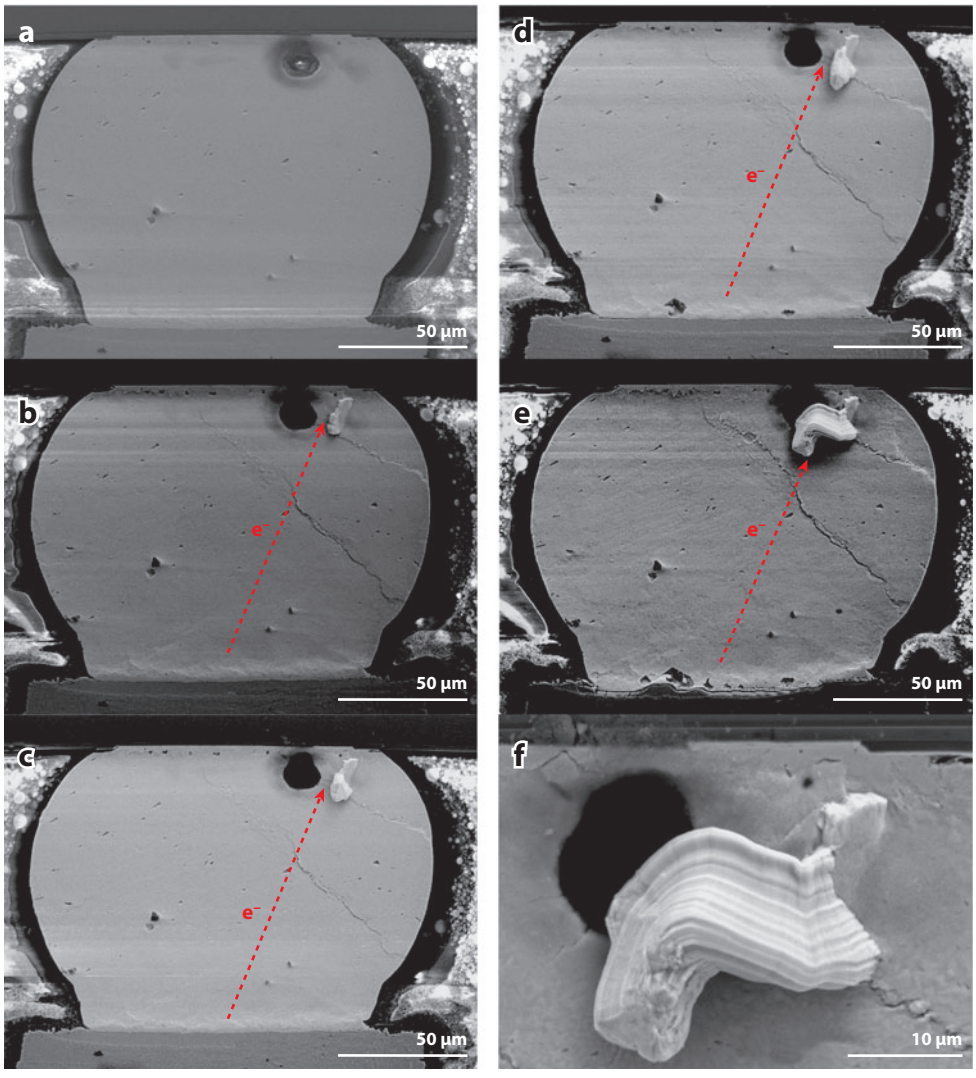

Figure 14

Scanning electron microscopy (SEM) images of a cross section of eutectic SnAgCu solder joints after (*a*) 0 h, (*b*) 38.5 h, (*c*) 68.5 h, (*d*) 99.5 h, and (*e*) 248.5 h. (*f*) An enlarged image of the whisker shows a rack of lines on the whisker surface. The results indicate that electromigration (EM) generates high stress at the cathode end of a solder bump.

surface morphology of whisker formation at the anode in a solder bump after stressing by 1.4×10^4 A cm^{-2} at 150°C for (*a*) 0 h, (*b*) 38.5 h, (*c*) 68.5 h, (*d*) 99.5 h, and (*e*) 248.5 h. The electrons were transported up into the solder bump and escaped from the upper-right corner. The important observation here is the very beginning of whisker initiation from a cracked surface. The results indicate that high stress is established during current stressing in flip-chip solder joints at relatively high temperatures. The back stress in SnAgCu appears larger than that in the eutectic SnPb solder (107), which may be attributed to Sn surface oxide in the SnAgCu solder.

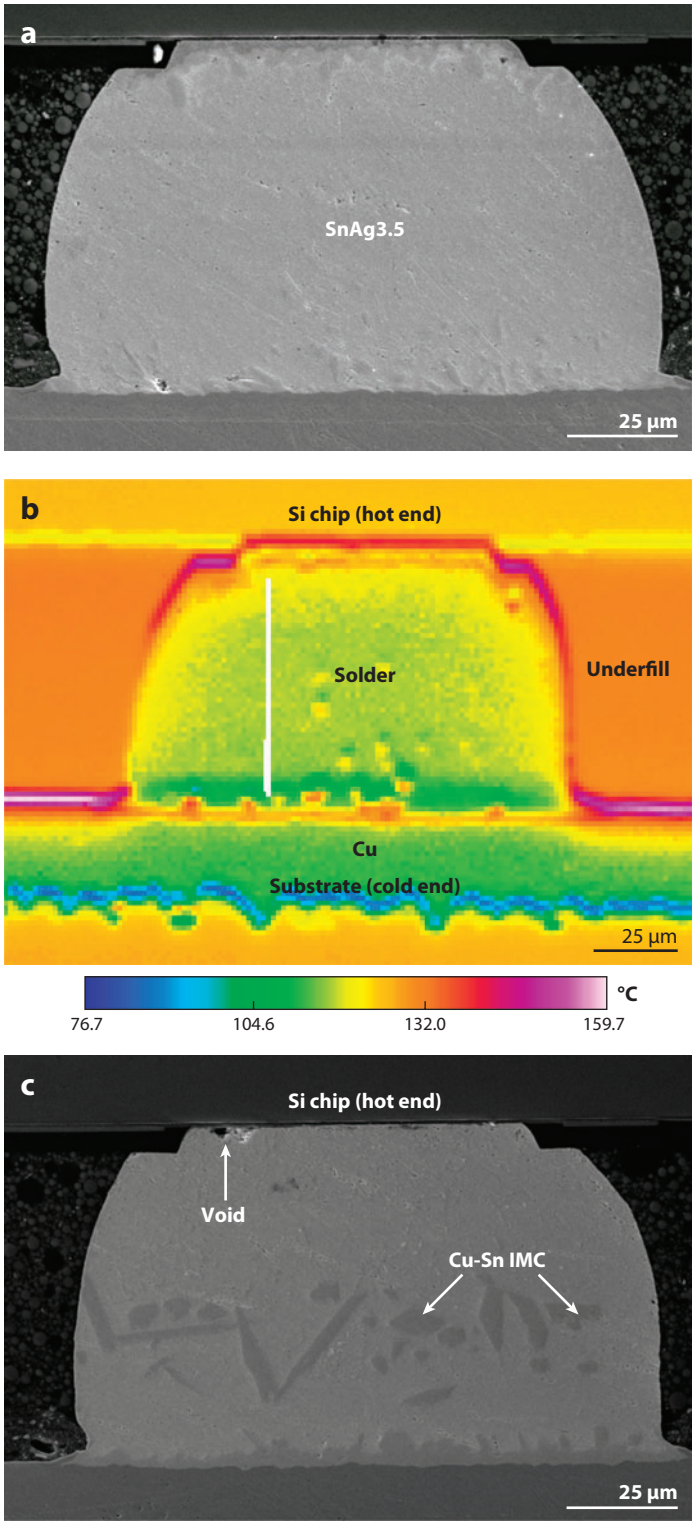

Figure 15

(*a*) Cross-sectional scanning electron microscopy (SEM) images representing the microstructure for an unpowered bump before a thermomigration (TM) test. (*b*) Temperature distribution measured by an infrared microscope when the neighboring bumps were stressed by 0.55 A at 150°C. The built-in thermal gradient was 1143°C cm^{-1} across the solder bump. (*c*) After the TM test for 60 h. The Cu UBM was dissolved completely due to TM of Cu to the cold (substrate) end. IMC denotes intermetallic compound.

6.4. Thermomigration of Cu and Ni in Flip-Chip Solder Joints

As described above, the dissolution of Cu and Ni in Pb-free solders is quite high, and the diffusion rates of Cu and Ni along the *c* axis of Sn crystals are very fast. The dissolution of Cu and Ni atoms may occur under a thermal gradient created during the EM process (111, 112). **Figure 15*a*** shows a eutectic SnAg solder bump with a 5-μm UBM on the chip side before a TM test. This bump was next to another bump that was under EM stressing at 0.55 A and 150°C. This joint had no current passing through it but possessed a thermal gradient of 1143°C cm^{-1}, as illustrated in **Figure 15*b***. After 60 h of the TM test, the Cu-Sn IMC migrated to the cold (substrate) end, as shown in **Figure 15*c***. Although this bump was unpowered, the damage is clear near the upper left corner, as indicated in **Figure 15*c***. The Cu UBM dissolved almost completely into the solder. This dissolution can be attributed to the TM of Cu atoms by fast interstitial diffusion and the reaction with Sn atoms to form Cu-Sn IMCs inside the solder bump. Therefore, the TM of Cu enhances Cu dissolution during the EM process, accelerating EM failure in Pb-free solder joints with Cu UBMs. How to mitigate this effect deserves further study.

7. CONCLUSIONS

We review here electromigration and TM in flip-chip solder joints and the damage caused due to these processes, emphasizing the effects of current crowding and Joule heating. Serious current-crowding and Joule heating effects play critical roles in the reliability failure mechanisms of solder joints. For solder joints with thin-film UBMs, voids initiate at the location with peak current density and with peak temperature. For solder joints with thick-film UBMs, the dissolution of UBM materials begins at a similar location and then gradually consumes the remaining UBMs. The bumps may become brittle after EM because of void and IMC formation. EM-enhanced dissolution of UBM materials will be the primary challenge for the continued use of Pb-free solder bumps.

DISCLOSURE STATEMENT

The authors are not aware of any affiliations, memberships, funding, or financial holdings that might be perceived as affecting the objectivity of this review.

ACKNOWLEDGMENTS

C.C. thanks the National Science Council of the ROC for the financial support through grant NSC96-2628-E-009-010-MY3. K.N.T. is grateful for support from NSF contract DMR 0503726 and Semiconductor Research Corporation contract KJ-1772. The authors thank Dr. Shih-Wei Liang at National Chiao Tung University for assistance in the preparation of figures and references.

LITERATURE CITED

1. Tu KN. 2003. Recent advances on electromigration in very-large-scale-integration of interconnects. *J. Appl. Phys.* 94:5451–73
2. Wright SL, Polastre R, Gan H, Buchwalter LP, Horton R, et al. 2006. Characterization of micro-bump C4 interconnects for Si-carrier SOP applications. *Proc. Electron. Compon. Technol. Conf., 56th, San Diego* 15:633–40
3. Tsui YK, Lee SWR. 2005. Design and fabrication of a flip-chip-on-chip 3-D packaging structure with a through-silicon via for underfill dispensing. *IEEE Trans. Adv. Packag.* 28:413–20

4. Brandenburg S, Yeh S. 1998. Electromigration studies of flip-chip solder bump solder joints. *Proc. Surf. Mt. Int. Conf. Exhib., San Jose, CA*, pp. 337–44
5. Liu CY, Chen C, Liao CN, Tu KN. 1999. Microstructure-electromigration correlation in a thin stripe of eutectic SnPb solder stressed between Cu electrodes. *Appl. Phys. Lett.* 75:58–60
6. Liu CY, Chen C, Tu KN. 2000. Electromigration in Sn-Pb solder strips as a function of alloy composition. *J. Appl. Phys.* 88:5703–9
7. Huynh QT, Liu CY, Chen C, Tu KN. 2001. Electromigration in eutectic SnPb solder lines. *J. Appl. Phys.* 89:4332–35
8. Zeng K, Tu KN. 2002. Six cases of reliability study of Pb-free solder joints in electronic packaging technology. *Mater. Sci. Eng. Rep.* 38:55–105
9. JEDEC Standard. 2008. *JEP154: Guideline for Characterizing Solder Bump Electromigration Under Constant and Temperature Stress*. Arlington, VA: JEDEC Solid State Technol. Assoc.
10. Yeh ECC, Tu KN. 2000. Numerical simulation of current crowding phenomena and their effects on electromigration in very large scale integration interconnects. *J. Appl. Phys.* 88:5680–86
11. Yeh ECC, Choi WJ, Tu KN, Elenius P, Balkan H. 2002. Current-crowding-induced electromigration failure in flip-chip solder joints. *Appl. Phys. Lett.* 80:580–82
12. Shao TL, Liang SW, Lin TC, Chen C. 2005. Three-dimensional simulation on current-density distribution in flip-chip solder joints under electric current stressing. *J. Appl. Phys.* 98:044509
13. Lai YS, Kao CL. 2006. Characteristics of current crowding in flip-chip solder bumps. *Microelectron. Reliab.* 46:915–22
14. Liang SW, Chang YW, Chen C. 2006. Effect of Al-trace dimension on Joule heating and current crowding in flip-chip solder joints under accelerated electromigration. *Appl. Phys. Lett.* 88:172108
15. Nah JW, Paik KW, Suh JO, Tu KN. 2003. Mechanism of electromigration-induced failure in the 97Pb-3Sn and 37Pb-63Sn composite solder joints. *J. Appl. Phys.* 94:7560–66
16. Chen CM, Huang CC. 2008. Atomic migration in eutectic SnBi solder alloys due to current stressing. *J. Mater. Res.* 23:1051–56
17. Jang JW, Ramanathan LN, Tang J, Frear DR. 2008. Secondary current crowding effect during electromigration of flip-chip solder joints. *J. Electron. Mater.* 37:185–88
18. Lu H, Yu C, Li PL, Chen JM. 2008. Current crowding and its effects on electromigration and interfacial reaction in lead-free solder joints. *J. Electron. Packag.* 130:031008
19. Yu C, Lu H, Fan RZ, Li SM. 2007. Factors influencing current density distribution and current crowding in flip-chip solder joints. *Sci. Technol. Weld. Join.* 12:423–30
20. Wang CH, Chen SW. 2006. Electric current effects in flip-chip solder joints. *J. Chin. Inst. Chem. Eng.* 37:185–91
21. Chiang KN, Lee CC, Lee CC, Chen KM. 2006. Current crowding-induced electromigration in SnAg3.0Cu0.5 microbumps. *Appl. Phys. Lett.* 88:072102
22. Zhang LY, Ou SQ, Huang J, Tu KN, Gee S, et al. 2006. Effect of current crowding on void propagation at the interface between intermetallic compound and solder in flip-chip solder joints. *Appl. Phys. Lett.* 88:012106
23. Liang SW, Chang YW, Shao TL, Chen C, Tu KN. 2006. Effect of 3-dimensional current and temperature distribution on void formation and propagation in flip-chip solder joints during electromigration. *Appl. Phys. Lett.* 89:022117
24. Chang YW, Liang SW, Chen C. 2006. Study of void formation due to electromigration in flip-chip solder joints using Kelvin bump probes. *Appl. Phys. Lett.* 89:032103
25. Lin YH, Hu YC, Tsai CM, Kao CR, Tu KN. 2005. In situ observation of the void formation-and-propagation mechanism in solder joints under current-stressing. *Acta Mater.* 53:2029–35
26. Liu CY, Chen JT, Chuang YC, Lin K, Wang SJ. 2007. Electromigration-induced Kirkendall voids at the Cu/Cu3Sn interface in flip-chip Cu/Sn/Cu joints. *Appl. Phys. Lett.* 90:112114
27. Yao Y, Keer LM, Fine ME. 2009. Electromigration effect on pancake type void propagation near the interface of bulk solder and intermetallic compound. *J. Appl. Phys.* 105:063710
28. Lee A, Ho CE, Subramanian KN. 2007. Electromigration induced microstructure and morphological changes in eutectic SnPb solder joints. *J. Mater. Res.* 22:3265–72

29. Gee S, Kelkar N, Huang J, Tu KN. 2005. Lead-free and SnPb bump electromigration testing. *Proc. InterPACK, July 17–22, San Francisco*, IPACK2005–73417
30. Ding M, Wang G, Chao B, Ho PS. 2006. Effect of contact metallization on electromigration reliability of Pb-free solder joints. *J. Appl. Phys.* 99:094906
31. Lin YL, Lai YS, Tsai CM, Kao CR. 2006. Effect of surface finish on the failure mechanisms of flip-chip solder joints under electromigration. *J. Electron. Mater.* 35:2147–53
32. Nah JW, Suh JO, Tu KN. 2005. Effect of current crowding and Joule heating on electromigration-induced failure in flip-chip composite solder joints tested at room temperature. *J. Appl. Phys.* 98:013715
33. Lee TY, Tu KN, Kuo SM, Frear DR. 2001. Electromigration of eutectic SnPb solder interconnects for flip-chip technology. *J. Appl. Phys.* 89:3189–94
34. Eaton DH, Rowatt JD, Dauksher WJ. 2006. Geometry effects on the electromigration of eutectic Sn/Pb flip-chip solder bumps. *Proc. IEEE Int. Reliab. Phys. Symp.*, pp. 243–49
35. Wu JD, Zheng PJ, Lee CW, Hung SC, Lee JJ. 2006. A study in flip-chip UBM/bump reliability with effects of SnPb solder composition. *Microelectron. Reliab.* 46:41–52
36. Jang JW, Ramanathan LN, Frear DR. 2008. Electromigration behavior of lead-free solder flip-chip bumps on NiP/Cu metallization. *J. Appl. Phys.* 103:123506
37. Ouyang FY, Tu KN, Kao CL, Lai YS. 2007. Effect of electromigration in the anodic Al interconnect on melting of flip-chip solder joints. *Appl. Phys. Lett.* 90:211914
38. Chiu SH, Chen C. 2006. Investigation of void nucleation and propagation during electromigration of flip-chip solder joints using X-ray microscopy. *Appl. Phys. Lett.* 89:262106
39. Liang SW, Chiu SH, Chen C. 2007. Effect of degradation of Al line on Joule heating of flip-chip solder joints. *Appl. Phys. Lett.* 90:082103
40. Yamanaka K, Tsukada Y, Suganuma K. 2007. Studies on solder bump electro-migration in Cu/Sn-3Ag-0.5Cu/Cu system. *Microelectron. Reliab.* 47:1280–87
41. Hsu YC, Shao TL, Yang CJ, Chen C. 2003. Electromigration study in SnAg3.8Cu0.7 solder joints on Ti/Cr-Cu/Cu under bump metallization. *J. Electron. Mater.* 32:1222–27
42. Choi WJ, Yeh ECC, Tu KN. 2003. Mean-time-to-failure study of flip-chip solder joints on Cu/Ni(V)/Al thin-film underbump-metallization. *J. Appl. Phys.* 94:5665–71
43. Lin YL, Chang CW, Tsai CM, Lee CW, Kao CR. 2006. Electromigration-induced UBM consumption and the resulting failure mechanisms in flip-chip solder joints. *J. Electron. Mater.* 35:1010–16
44. Chang YW, Chiang TH, Chen C. 2007. Effect of void propagation on bump resistance due to electromigration in flip-chip solder joints using Kelvin structure. *Appl. Phys. Lett.* 91:132113
45. Yang D, Chan YC, Tu KN. 2008. The time-dependent melting failure in flip-chip lead-free solder interconnects under current stressing. *Appl. Phys. Lett.* 93:041907
46. Lin YL, Lai YS, Lin YW, Kao CR. 2008. Effect of UBM thickness on the mean time to failure of flip-chip solder joints under electromigration. *J. Electron. Mater.* 37:96–101
47. Alfred Y, Bernd E, Charles L. 2008. Consideration of temperature and current stress testing on flip-chip solder interconnects. *Microelectron. Reliab.* 48:1847–56
48. Tsai CM, Lin YL Tsai JY, Lai YS, Kao CR. 2006. Local melting induced by electromigration in flip-chip solder joints. *J. Electron. Mater.* 35:1005–9
49. Miyazaki T, Omata T. 2006. Electromigration degradation mechanism for Pb-free flip-chip micro solder bumps. *Microelectron. Reliab.* 46:1898–903
50. Huang AT, Tu KN, Lai YS. 2006. Effect of the combination of electromigration and thermomigration on phase migration and partial melting in flip-chip composite SnPb solder joints. *J. Appl. Phys.* 100:033512
51. Deleted in proof
52. Prigogine I. 1995. *Introduction to Thermodynamics of Irreversible Processes*. Springfield, IL: CC Thomas
53. Liang SW, Chang YW, Chen C. 2006. Geometrical effect of bump resistance measurement by Kelvin structure. *J. Electron. Mater.* 35:1647–54
54. Ye H, Basaran C, Hopkins D. 2003. Thermomigration in Pb-Sn solder joints under Joule heating during electric current stressing. *Appl. Phys. Lett.* 82:1045–47
55. Chiu SH, Shao TL, Chen C, Yao DJ, Hsu CY. 2006. Infrared microscopy of hot spots induced by Joule heating in flip-chip SnAg solder joints under accelerated electromigration. *Appl. Phys. Lett.* 88:022110

56. Shao TL, Chen YH, Chiu SH, Chen C. 2004. Electromigration failure mechanisms for SnAg3.5 solder bumps on Ti/Cr-Cu/Cu and Ni(P)/Au metallization pads. *J. Appl. Phys.* 96:4518–24
57. Alam MO, Wu BY, Chan YC, Tu KN. 2006. High electric current density-induced interfacial reactions in micro ball grid array (mBGA) solder joints. *Acta Mater.* 54:613–21
58. Hsiao HY, Liang SW, Ku MF, Chen C, Yao DJ. 2008. Direct measurement of hot-spot temperature in flip-chip solder joints under current stressing using infrared microscopy. *J. Appl. Phys.* 104:033708
59. Liang SW, Chang YW, Chen C. 2007. Three-dimensional thermoelectrical simulation in flip-chip solder joints with thick underbump metallizations during accelerated electromigration testing. *J. Electron. Mater.* 36:159–67
60. Huang AT, Gusak AM, Tu KN. 2006. Thermomigration in SnPb composite flip-chip solder joints. *Appl. Phys. Lett.* 88:141911
61. Chuang YC, Liu CY. 2006. Thermomigration in eutectic SnPb alloy. *Appl. Phys. Lett.* 88:174105
62. Hsiao HY, Chen C. 2007. Thermomigration in flip-chip SnPb solder joints under alternating current stressing. *Appl. Phys. Lett.* 90:152105
63. Gu X, Chan YC. 2009. Thermomigration and electromigration in Sn58Bi solder joints. *J. Appl. Phys.* 105:093537
64. Hsiao HY, Chen C. 2009. Thermomigration in Pb-free SnAg solder joint under alternating current stressing. *Appl. Phys. Lett.* 94:092107
65. Abdulhamid MF, Basaran C. 2009. Influence of thermomigration on lead-free solder joint mechanical properties. *J. Electron. Packag.* 131:011002
66. Yang D, Chan YC, Wu BY, Pecht M. 2008. Electromigration and thermomigration behavior of flip-chip solder joints in high current density packages. *J. Mater. Res.* 23:2333–39
67. Basaran C, Li SD, Abdulhamid MF. 2008. Thermomigration induced degradation in solder alloys. *J. Appl. Phys.* 103:123520
68. Lee JH, Lim GT, Yang ST, Suh MS, Chung QH, et al. 2008. Electromigration and thermomigration characteristics in flip-chip Sn-3.5Ag solder bump. *J. Korean Inst. Metals Mater.* 46:310–14
69. Yang D, Wu BY, Chan YC, Tu KN. 2007. Microstructural evolution and atomic transport by thermomigration in eutectic tin-lead flip-chip solder joints. *J. Appl. Phys.* 102:043502
70. Chuang YC, Liu CY. 2007. The effect of thermomigration on phase coarsening in eutectic SnPb alloy. *J. Electron. Mater.* 36:1495–500
71. Li SD, Abdulhamid MF, Basaran C. 2009. Damage mechanics of low temperature electromigration and thermomigration. *IEEE Trans. Adv. Packag.* 32:478–85
72. Yang D, Alam MO, Wu BY, Chan YC. 2006. Thermomigration in eutectic tin-lead flip chip solder joints. *Proc. Electron. Packag. Technol. Conf., 8th, Singapore*, pp. 565–69
73. Ebersberger B, Bauer R, Alexa L. 2005. Reliability of lead-free SnAg solder bumps: influence of electromigration and temperature. *Proc. Electron. Compon. Technol. Conf., 55th, Orlando* 2:1407–15
74. Yang D, Wu BY, Chan YC, Tu KN. 2007. Microstructural evolution and atomic transport by thermomigration in eutectic SnPb flip-chip solder joints. *J. Appl. Phys.* 102:043502
75. Huntington HB, Grone AR. 1961. Current-induced marker motion in gold wires. *J. Phys. Chem. Solids* 20:76–87
76. Balluffi RW, Allen SM, Carter WC, eds. 2005. *Kinetics of Materials*. Hoboken, NJ: Wiley-Intersci.
77. Lai YS, Chiu YT, Chen J. 2008. Electromigration reliability and morphologies of Cu pillar flip-chip solder joints with Cu substrate pad metallization. *J. Electron. Mater.* 37:1624–30
78. Ebersberger B, Lee C. 2008. Cu pillar bumps as a lead-free drop-in replacement for solder-bumped, flip-chip interconnects. *Electron. Compon. Technol. Conf., 58th, Lake Buena Vista, FL*, pp. 59–66
79. Hsu HJ, Huang JT, Chao PS, Shih SH. 2008. Surface modification on plating-based Cu/Sn/0.7Cu lead-free copper pillars by using polishing. *Microelectron. Eng.* 85:1590–96
80. Jinhua Y, Anand A, Mui Y, Srinivasan P, Master R. 2007. Reliability study on copper pillar bumping with lead free solder. *Electron. Packaging Technol. Conf., 9th*, pp. 618–22
81. Ate H, Osborn T, Allen SAB, Kohl PA. 2006. Low-temperature bonding of copper pillars for all-copper chip-to-substrate interconnections. *Electrochem. Solid-State Lett.* 9:C192–95
82. Nah JW, Suh JO, Tu KN, Seung WY, Rao VS, et al. 2006. Electromigration in flip-chip solder joints having a thick Cu column bump and a shallow solder interconnect. *J. Appl. Phys.* 100:123513

83. Liao EB, Tay AAO, Ang ST, Feng HH, Nagarajan R, Kripesh V. 2006. Fatigue and bridging study of high-aspect-ratio multicopper-column flip-chip interconnects through solder joint shape modeling. *IEEE Trans. Compon. Packag. Technol.* 29:560–69
84. Liang SW, Chang YW, Chen C. 2007. Relieving hot-spot temperature and current crowding effect during electromigration in solder bumps by using Cu columns. *J. Electron. Mater.* 36:1348–54
85. Nah JW, Chen K, Tu KN, Su BR, Chen C. 2007. Mechanism of electromigration-induced failure in flip-chip solder joints with a 10 micron thick Cu underbump-metallization. *J. Mater. Res.* 22:763–69
86. Lin CT, Chuang YC, Wang SJ, Liu CY. 2006. Current density dependence of electromigration-induced flip-chip Cu pad consumption. *Appl. Phys. Lett.* 89:101906
87. Liu CY, Ke L, Chuang YC, Wang SJ. 2006. Study of electromigration-induced Cu consumption in the flip-chip Sn/Cu solder bumps. *J. Appl. Phys.* 100:083702
88. Xu LH, Han JK, Liang JJ, Tu KN, Lai YS. 2008. Electromigration induced high fraction of compound formation in SnAgCu flip-chip solder joints with copper column. *Appl. Phys. Lett.* 92:262104
89. Orchard HT, Greer AL. 2005. Electromigration effects on compound growth at interfaces. *Appl. Phys. Lett.* 86:231906
90. Kim HK, Tu KN. 1995. Rate of consumption of Cu soldering accompanied by ripening. *Appl. Phys. Lett.* 67:2002–4
91. Chao B, Chae SH, Zhang XF, Lu KH, Ding M, et al. 2006. Electromigration enhanced intermetallic growth and void formation in Pb-free solder joints. *J. Appl. Phys.* 100:084909
92. Chao BHL, Zhang XF, Chae SH, Ho PS. 2009. Recent advances on kinetic analysis of electromigration enhanced intermetallic growth and damage formation in Pb-free solder joints. *Microelectron. Reliab.* 49:253–63
93. Chao BHL, Chae SH, Zhang XF, Lu KH, Im J, Ho PS. 2007. Investigation of diffusion and electromigration parameters for Cu-Sn intermetallic compounds in Pb-free solders using simulated annealing. *Acta Mater.* 55:2805–14
94. Kuo SM, Lin KL. 2007. Microstructure evolution during electromigration between Sn-9Zn solder and Cu. *J. Mater. Res.* 22:1240–49
95. Chae SH, Zhang XF, Lu KH, Chao BHL, Ho PS, et al. 2007. Electromigration statistics and damage evolution for Pb-free solder joints with Cu and Ni UBM in plastic flip-chip packages. *J. Mater. Sci.-Mater. Electron.* 18:247–58
96. Chen SW, Lin SK, Jao JM. 2004. Electromigration effects upon interfacial reactions in flip-chip solder joints. *Mater. Trans.* 45:661–65
97. Ren F, Nah JW, Tu KN, Xiong B, Xu LH, Pang JHL. 2006. Electromigration induced ductile-to-brittle transition in lead-free solder joints. *Appl. Phys. Lett.* 89:141914
98. Zhang L, Wang ZG, Shang JK. 2007. Current-induced weakening of Sn3.5Ag0.7Cu Pb-free solder joints. *Scr. Mater.* 56:381–84
99. Nah JW, Ren F, Paik KW, Tu KN. 2006. Effect of electromigration on mechanical shear behavior of flip-chip solder joints. *J. Mater. Res.* 21:698–702
100. Kinney C, Morris JW, Lee TK, Liu KC, Xue J, Towne D. 2009. The influence of an imposed current on the creep of Sn-Ag-Cu solder. *J. Electron. Mater.* 38:221–26
101. Xu LH, Pang JHL, Ren F, Tu KN. 2006. Electromigration effect on intermetallic growth and Young's modulus in SAC solder joint. *J. Electron. Mater.* 35:2116–25
102. Lu M, Shih DY, Lauro P, Goldsmith C, Henderson DW. 2008. Effect of Sn grain orientation on electromigration degradation mechanism in high Sn-based Pb-free solders. *Appl. Phys. Lett.* 92:211909
103. Dyson BF, Anthony TR, Turnbull D. 1967. Interstitial diffusion of copper in tin. *J. Appl. Phys.* 38:3408
104. Yeh DC, Huntington HB. 1984. Extreme fast-diffusion system: nickel in single-crystal tin. *Phys. Rev. Lett.* 53:1469–72
105. Xu LH, Pang JHL, Tu KN. 2006. Effect of electromigration-induced back stress gradient on nanoindentation marker movement in SnAgCu solder joints. *Appl. Phys. Lett.* 89:221909
106. Wu BY, Chan YC, Zhong HW, Alam MO, Lai JKL. 2007. Study of the thermal stress in a Pb-free half-bump solder joint under current stressing. *Appl. Phys. Lett.* 90:232112
107. Ouyang FY, Chen K, Tu KN, Lai YS. 2007. Effect of current crowding on whisker growth at the anode in flip-chip solder joints. *Appl. Phys. Lett.* 91:231919

108. Zhang JS, Xi HJ, Wu YP, Wu FS. 2009. Thermomechanical stress and strain in solder joints during electromigration. *J. Electron. Mater.* 38:678–84
109. Ogurtani TO, Akyildiz O. 2008. Morphological evolution of voids by surface drift diffusion driven by the capillary, electromigration, and thermal-stress gradient induced by the steady state heat flow in passivated metallic thin films and flip-chip solder joints. II. Applications. *J. Appl. Phys.* 104:023522
110. Yoon MS, Ko MK, Kim BN, Kim BJ, Park YB, Joo YC. 2008. Line length dependence of threshold current density and driving force in eutectic SnPb and SnAgCu solder electromigration. *J. Appl. Phys.* 103:073701
111. Chen HY, Chen C, Tu KN. 2008. Failure induced by thermomigration of interstitial Cu in Pb-free flip-chip solder joints. *Appl. Phys. Lett.* 93:122103
112. Jen MHR, Liu LC, Lai YS. 2009. Electromigration test on void formation and failure mechanism of FCBGA lead-free solder joints. *IEEE Trans. Adv. Packag.* 32:79

Annual Review of
Materials Research

Volume 40, 2010

Contents

New Developments in Composite Materials

Current Interest